ELSEVIER

European Journal of Pharmacology 416 (2001) 33–41

ejp

www.elsevier.nl/locate/ejphar

Ligand induced conformational states of the 5-HT_{1A} receptor

Ingebrigt Sylte [a,*], Agnieszka Bronowska [b], Svein G. Dahl [a]

[a] *Department of Pharmacology, Institute of Medical Biology, Faculty of Medicine, University of Tromsø, N-9037 Tromsø, Norway*
[b] *Department of Chemistry, University of Warsaw, Pasteura 1, 02-093 Warsaw, Poland*

Received 26 October 2000; received in revised form 12 February 2001; accepted 16 February 2001

Abstract

It has been shown that G-protein coupled receptors have seven transmembrane α-helices, but the structural changes occurring in a G-protein coupled receptor as a response on agonist stimulus and the molecular events leading to blockade of the signal transduction by antagonists are not well understood. In the present study, the AMBER 5.0 force field was used for comparative molecular dynamics simulations of a 5-HT_{1A} receptor model in the absence of ligand, in complex with a 5-HT_{1A} receptor agonist (*R*)-8-hydroxy-2-(di-*n*-propylamino)tetralin [(*R*)-8-OH-DPAT], in complex with a selective 5-HT_{1A} receptor antagonist (*S*)-*N*-*tert*-butyl-3-[4-(2-methoxyphenyl)piperazin-1-yl]-2-phenylpropanamide [(*S*)-WAY100135], and in complex with the partial agonist, buspirone. In the simulations, the agonist induced larger conformational changes into transmembrane helix 3 and 6 than into the other helices, while the main conformational differences between the agonist bound receptor and the antagonist bound receptor were in transmembrane helix 5 and 6. During the simulations, all the three ligands constrained the helical movements compared to those observed in the receptor without any ligand.

Keywords: G-protein coupled receptor; Molecular dynamics; Receptor activation; Conformational changes, ligand induced

1. Introduction

The rhodopsin family of G-protein coupled receptors constitute a large superfamily of membrane proteins that transduce signals across the cell membrane by receiving a ligand stimulus at the external side and activation of a G-protein at the cytosolic side. The structural changes that occur in the receptor upon external agonist stimulation and the molecular events leading to blockade of the signal transduction by antagonists are poorly understood.

A classical model of receptor activation proposes that G-protein coupled receptors can exist in equilibrium between two inter-convertible allosteric states R and R^* (Scheer and Cotecchia, 1997). In the absence of ligand, the inactive state R predominates, while the presence of an agonist stabilises the receptor in the active R^* conformation. However, studies have demonstrated that many G-protein coupled receptors are capable of interacting with several distinct signalling pathways, and may generate different agonist induced pharmacological effects depending on the signalling pathway (Perez et al., 1996; Sidhu and Niznik, 2000). This indicates that the receptor may exist in several activated conformational states. Knowledge about the relationship between the structure of the ligand and the ligand-induced conformational states of the receptor is important in order to enable design of new ligands interfering with specific signalling pathways.

The 5-HT_{1A} receptor belongs to the class of G_i/G_o coupled inhibitory receptors. Via G-protein interactions activation of the 5-HT_{1A} receptors inhibits adenylyl cyclase activity and the production of adenosine 3′,5′-cyclic monophosphate (cAMP), increases the potassium conductance by regulating inward rectifying K^+ channels (GIRK-channels) and decreases the opening of voltage gated Ca^{2+} channels (Barnes and Sharp, 1999). Full agonists induced a 5-HT_{1A} receptor conformation that activated $G_{i\alpha-1}$, $G_{i\alpha-2}$ and $G_{i\alpha-3}$ subunits in HeLa and chinese hamster ovary fibroblast cells (CHO-K1 cells) (Fargin et al., 1991; Raymond et al., 1993), while the partial agonists induced a receptor conformation with lower affinity for $G_{i\alpha-2}$ and $G_{i\alpha-3}$ subunits in CHO-K1 cells (Gettys et al., 1994).

Recently, an X-ray crystal structure of rhodopsin at 2.8 Å resolution was reported (Palczewski et al., 2000). This is the first experimental structure of a G-protein coupled

* Corresponding author. Tel.: +47-77-644-705; fax: +47-77-645-310.
E-mail address: sylte@fagmed.uit.no (I. Sylte).

0014-2999/01/$ - see front matter
PII: S0014-2999(01)00860-3

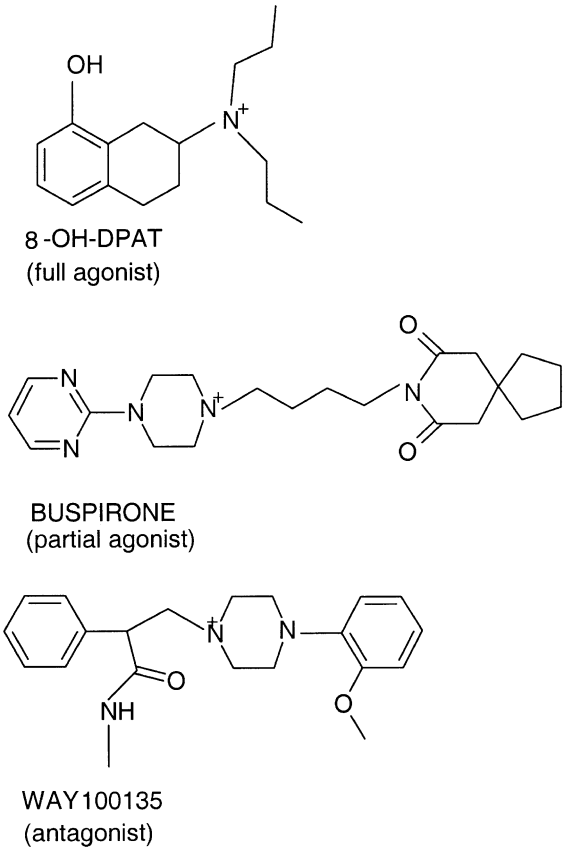

Fig. 1. Chemical structure of the ligand molecules.

receptor that has been reported at atomic resolution. The organisation of the seven transmembrane helices confirm the suggested α-carbon template for the transmembrane helices in the rhodopsin family of G-protein coupled receptors (Baldwin et al., 1997). In the present study, a model of the human 5-HT_{1A} receptor was constructed and used for comparative molecular dynamics simulations of the receptor in absence of ligand, in a complex with the 5-HT_{1A} receptor agonist, (*R*)-8-hydroxy-2-(di-*n*-propylamino)tetralin [(*R*)-8-OH-DPAT] (Arvidsson et al., 1981), in complex with a selective 5-HT_{1A} receptor antagonist, (*S*)-*N*-*tert*-butyl-3-[4-(2-methoxyphenyl)piperazin-1-yl]-2-phenylpropanamide [(*S*)-WAY100135] (Cliffe et al., 1993), and in complex with the partial agonist, buspirone (Peroutka, 1995) (Fig. 1). The receptor model was constructed based on an electron cryo-microscopy structure of rhodopsin (Unger et al., 1997), a general α-carbon atom template for the transmembrane helical part of G-protein coupled receptors (Baldwin et al., 1997), and loop structures available in the Protein Data Bank (http://www.rcsb.org/pdb/).

2. Materials and methods

All calculations were performed with the AMBER 5.0 programs using the Cornell et al. (1995) force field. Water molecules were not included in the calculations, and a dielectric constant of 4 and a distance dependent dielectric function was used. The use of a dielectric constant of 4 and a distance dependent dielectric function has been found to satisfactory reproduce the X-ray crystal structures of soluble proteins without including water molecules (Christensen and Jørgensen, 1997). To preserve the helical conformation of transmembrane helices during molecular dynamics simulations, constraint forces (corresponding to 5 kcal/mol) were applied between the backbone oxygen atom of residue n and the backbone nitrogen atom of residues $n + 4$, excluding prolines. Initial simulations indicated that intrahelical constraint forces corresponding to 5 kcal/mol were important for producing rigid helix body motions as observed in experimental studies (Farrens et al., 1996; Liu et al., 1996). A similar strategy for constraining the transmembrane helices together with a dielectric constant of $\varepsilon = 4$ and distance dependent dielectric function has also been used previously during molecular dynamics simulations of G-protein coupled receptor models (Fanelli et al., 1998).

Convergence criteria for molecular mechanical energy minimisation of ligand molecules and for receptor complexes: a root mean square (RMS) difference for the norm of the energy gradient between successive steps of 0.02 kcal/mol Å. Atomic restrained electrostatic potential (RESP) charges (Bayly et al., 1993) were calculated for the ligand molecules using a 6–31 G* basis set.

2.1. Construction of the receptor model

The model was constructed from our previous model of the 5-HT_{1A} receptor (Sylte et al., 1997). The helical bundle was adjusted according to the most resent low resolution structure of frog rhodopsin (Unger et al., 1997), and the suggested α-carbon template for the transmembrane helices in the rhodopsin family of G-protein coupled receptors (Baldwin et al., 1997). This resulted in a transmembrane helical bundle with transmembrane helix 3 being more in the centre of the helical bundle, and with transmembrane helix 3 and 5 more tilted than in our previous 5-HT_{1A} receptor model. The N-terminal structure was taken directly from our previous 5-HT_{1A} receptor model (Sylte et al., 1997), while initial backbone conformations of the extracellular loops, the first and second intracellular loops, and the C-terminal were constructed by searching for loop segments in the Protein Data Bank (http://www.rcsb.org/pdb/). The five loop conformations in the database with highest amino acid sequence homology with each of these receptor segments were inspected visually for the possibility of steric interactions with its local environment on the receptor. The loop conformation with most reasonable interactions and smallest deviation at the terminal ends were selected, and initial structures of the receptor segments were constructed by changing the side

chains of the loop conformation into the side chains of the corresponding receptor segment. An initial model of the third intracellular loop was constructed using a combination of secondary structure predictions by the PredictProtein server (http://dodo.cpmc.colombia.edu/pp/), and by searching for loop segments on the Protein Data Bank. The loops and terminals were connected to the helical bundle, and the receptor model was energy refined in several steps: (1) 25 ps of molecular dynamics simulation at 300 K with the helical bundle at fixed position; (2) 25 ps of molecular dynamics simulation at 300 K of all side chains in the model; (3) energy minimisation of the entire receptor. A disulphide bridge between Cys^{109} in transmembrane helix 3 and Cys^{187} in the second extracellular loop was present during all calculations.

2.2. Docking of (R)-8-OH-DPAT

A bioactive conformation of (*R*)-8-OH-DPAT has been suggested based on ligand fitting models (Hibert et al., 1989; Mellin et al., 1991) and structure-affinity relationships of amino tetralines (Kuiper et al., 1994). In this conformation, the basic nitrogen atom is positioned equatorial at the tetraline ring, the tetraline ring is in a half-chair conformation, the torsional angle $H_{C_2}–C_2–N–H_N$ is at about 180°, while the propyl C_α-atoms are approximately in the plane of the aromatic ring. All these criteria are satisfied in the X-ray crystal structure of (*R*)-8-OH-DPAT (Karlsson et al., 1988). Our previous modelling study of aminotetralines interacting with the 5-HT_{1A} receptor (Sylte et al., 1996), and the results of site directed mutagenesis experiments of the 5-HT_{1A} receptor (Guan et al., 1992; Ho et al., 1992; Chanda et al., 1993) were used as guidelines to dock the energy minimised crystal structure of (*R*)-8-OH-DPAT into a putative active site. The protonated amino group was in the direction of Asp^{116} and the hydroxyl group in the direction of amino acid residues in transmembrane helix 5. The complex was energy minimised until convergence and used as an initial complex for molecular dynamics simulations.

2.3. Docking of (S)-WAY100135

An initial model of (*S*)-*N*-*tert*-butyl-3-(4-(2-methoxyphenyl)-piperazine-1-yl]-2-phenylpropanamide [(*S*)-WAY100135] was generated from the X-ray crystal structure of buspirone (Chilmonczyk et al., 1995) and fragments in the Cambridge structural database. The initial model was energy minimised until convergence, and the energy minimised structure was used as a start structure for 400 ps of molecular dynamics simulation at 300 K. Bonds involving hydrogen atoms were constrained using the SHAKE-option. A pharmacophore model for 5-HT_{1A} antagonism suggests a nitrogen atom located about 5.6 Å from the centre of an aromatic ring, with a deviation of 1.6 Å from the ring plane (Hibert et al., 1988). The different conformers obtained during the simulation were energy minimised and compared with the pharmacophore model for 5-HT_{1A} receptor antagonism. The conformer with lowest potential energy among those in agreement with 5-HT_{1A} antagonist pharmacophore model was docked into the 5-HT_{1A} receptor model in several different positions. Six different receptor–(*S*)-WAY100135 complexes were energy minimised until convergence. The complexes were evaluated according to interaction energies between (*S*)-WAY100135 and the receptor, total potential energy of the complex and potential energy of the receptor. The most favourable complex was used as a start complex for 350 ps of molecular dynamics simulations.

2.4. Docking of buspirone

A previous docking study of buspirone analogues interacting with the 5-HT_{1A} receptor indicated that the rank order of ligand binding affinities was reproduced by calculations of receptor-binding energies when the imide moieties interacted with amino acids in transmembrane helix 3 and 7, while the quinolinyl part of ligands interacted with amino acids in transmembrane helix 6 (Sylte et al., 1997). The carbonyl oxygens of buspirone interacted with the side chains of Ser^{86} (transmembrane helix 2) and Ser^{393} (transmembrane helix 7). The energy minimised crystal structure of Buspirone (Chilmonczyk et al., 1995) was docked into the present model of the 5-HT_{1A} receptor in a similar position, the complex was energy minimised and used as an initial structure for 350 ps of molecular dynamics simulation.

2.5. Molecular dynamics of receptor–ligand interactions

Molecular dynamics simulations were performed for:

1. the receptor model alone;
2. the receptor–(*R*)-8-OH-DPAT complex;
3. the receptor–buspirone complex;
4. the receptor–(*S*)-WAY100135 complex.

The cut-off radius for non-bonded interactions was 12 Å, with a secondary cut-off radius of 15 Å. Bonds involving hydrogen atoms were constrained using the SHAKE option. The simulations were performed for 350 ps. The step length was 0.001 ps, and the non-bonded pair list was updated every 10 step during the simulation. The molecular system was gradually heated to 300 K during 0–30 ps and kept at 300 K for the rest of the simulation. Coordinates saved every 1.0 ps during 150–350 ps of simulation were used to calculate an average structure of complexes from the simulations. The average structure was energy minimised until convergence.

The RMS of receptor domain fluctuations were calculated for the period between 150 and 350 ps, and the RMS

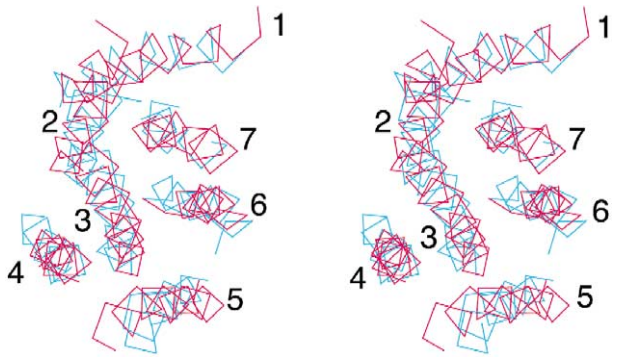

Fig. 2. Stereo illustration showing the TMH Cα traces of rhodopsin (blue) and the 5-HT_{1A} receptor model (red), viewed from the synaptic side.

differences of receptor domains between the four energy minimised average receptor structures were calculated.

3. Results

3.1. Structural similarities with the experimental model of rhodopsin

As indicated in Fig. 2, the helical packing in the 5-HT_{1A} receptor model was very similar to that in the experimental model of rhodopsin. Amino acid residues in the transmembrane helices, being highly conserved in the rhodopsin family of G-protein coupled receptors, were located in similar positions and had similar conformation. The atomic distance between the Cα-carbon atoms of highly conserved amino acids in the rhodopsin family also demonstrated spatial similarities in the helical bundle (Table 1). In both models, the acid residue in the E/DRY-motif at the intracellular end of transmembrane helix 3 formed a salt bridge with the basic residue in the motif. The largest divergences in the helical bundle were seen downstream of proline residues, since prolines in the rhodopsin structure induced larger kinks than in the 5-HT_{1A} receptor model.

Table 1
Distances between the Cα-atoms of amino acids in the experimental model of rhodopsin and the theoretical model of the 5-HT_{1A} receptor. Highly conserved amino acids in the rhodopsin family of G-protein coupled receptors are included. The amino acid numbering in the 5-HT_{1A} receptor is used in the table

Amino acid residues		Atomic distance	
		5-HT_{1A} model (Å)	Rhodopsin structure (Å)
Asn^{54}(TMH1)	Asp^{82}(TMH2)	7.5	6.6
Asn^{54}(TMH1)	Asn^{396}(TMH7)	9.3	8.7
Asp^{82}(TMH2)	Asn^{396}(TMH7)	7.8	8.9
Asn^{54}(TMH1)	Trp^{161}(TMH4)	18.5	17.8
Asp^{82}(TMH2)	Trp^{161}(TMH4)	15.6	16.9
Asn^{54} (TMH1)	Pro^{207}(TMH5)	24.9	24.4
Asn^{54}(TMH1)	Pro^{360}(TMH6)	23.5	23.8

The RMS differences between the backbone atoms in the transmembrane helices of the theoretical 5-HT_{1A} model and the experimental rhodopsin model were 3.0 Å.

3.2. Ligand–receptor contacts after simulation

Amino acid residues having van der Waals contact with the ligands in the average complexes after molecular dynamics simulations (Fig. 3) are shown in Table 2. The

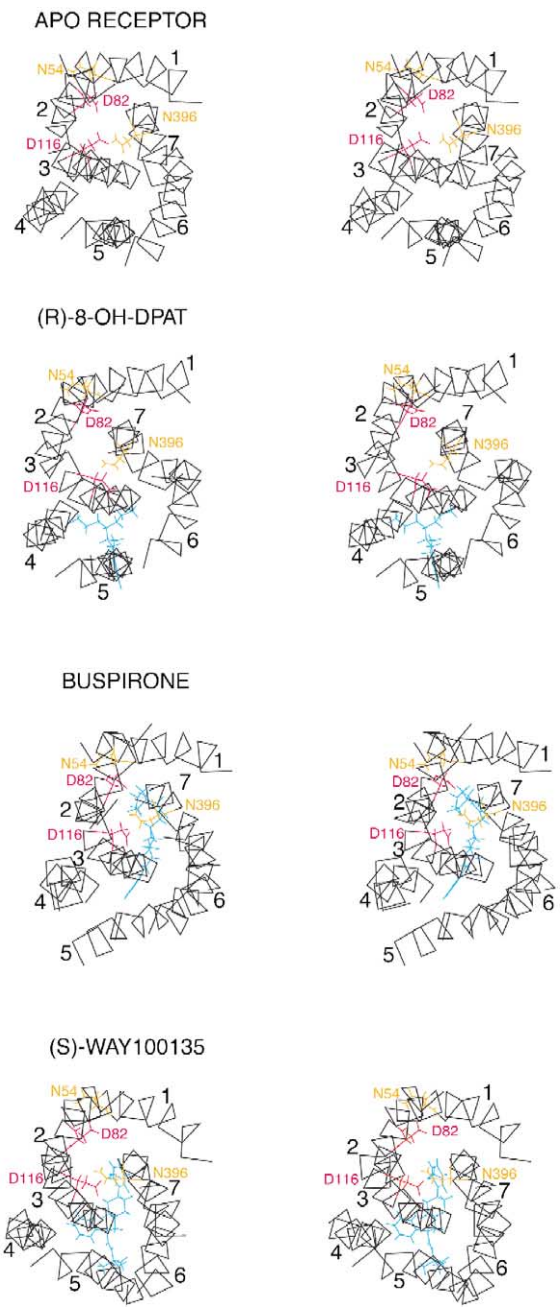

Fig. 3. Stereo illustration showing the energy minimized average receptor structures (150–350 ps). The Cα trace of TMHs and the side chains important for receptor function are shown. The receptor structures are viewed from the synaptic side.

Table 2
Amino acids having van der Waals contact with the ligands in the energy minimised average complexes (150–350 ps of simulation)

Ligand	Receptor domain	Amino acid residue
(*R*)-8-OH-DPAT	TMH3	Ile^{113}, Asp^{116}, Val^{117}
	TMH4	Met^{170}, Gly^{174}, Trp^{175}
	TMH5	Thr^{196}, Ser^{199}, Thr^{200}
	TMH6	Leu^{366}
	TMH7	Ile^{385}, Asn^{386}
Buspirone	TMH1	Leu^{43}
	TMH2	Leu^{88}, Val^{89}
	TMH3	Phe^{112}, Ile^{113}, Asp^{116}, Val^{117}
	TMH6	Phe^{361}, Pro^{369}
	TMH7	Ile^{385}, Asn^{386}, Gly^{389}, Tyr^{390}, Ser^{393}
(*S*)-WAY100135	TMH2	Met^{92}
	TMH3	Ile^{113}, Asp^{116}, Val^{117}
	TMH5	Ser^{199}, Ala^{203}
	TMH6	Phe^{362}, Ala^{365}
	TMH7	Ile^{385}, Asn^{386}, Gly^{389}, Tyr^{390}

positions of all ligands relative to the receptor were very similar to that before the molecular dynamics simulation.

In the average structure after simulation, the tetraline ring moiety of (*R*)-8-OH-DPAT (Fig. 1) interacted with amino acids in transmembrane helix 5 and 6, while the protonated dipropylamino group interacted with amino acids in transmembrane helix 3, 4, 6 and 7 (Fig. 3).

In the average structure after molecular dynamics simulation, the protonated piperazine ring in (*S*)-WAY10035 (Fig. 1) interacted with Asp^{116} and other amino acids in transmembrane helix 3, while the *N-tert*-butyl group interacted with amino acids in transmembrane helix 5 and 6. The methoxyphenyl ring interacted with amino acids in transmembrane helix 7 and with Met^{92} in transmembrane helix 2, while the phenyl ring interacted with amino acids in transmembrane helix 3 and 5 (Fig. 3).

After simulation, the imide ring system of buspirone (Fig. 1) interacted with amino acids in transmembrane helix 1, 2, 3 and 7 (Fig. 3). The pyrimidine ring interacted with amino acids in transmembrane helix 3 and 6, and the piperazine ring interacted with amino acids in transmembrane helix 3 and 7 (Fig. 3).

Site directed mutagenesis studies have shown that the side chain of Asn^{386} (transmembrane helix 7) is important for binding of pindolol but not of buspirone and (*R*)-8-OH-DPAT to the 5-HT_{1A} receptor (Guan et al., 1992). On the other hand, all ligands had van der Waals contact with Asn^{386} after the simulations (Table 2). However, (*R*)-8-OH-DPAT and buspirone interacted directly with the backbone of Asn^{386}, independently of its side chain, and these interactions should therefore be unaffected by mutations of the side chain.

3.3. Ligand induced conformational changes of the receptor

The RMS differences between specific receptor domains of the average receptor structures (150–350 ps) are shown in Table 3. The largest RMS differences in the transmembrane helices between the apo receptor and the (*R*)-8-OH-DPAT bound receptor were in transmembrane helix 3 and 6, while the largest RMS differences in the transmembrane helices after simulation with buspirone and in absence of ligand were in transmembrane helix 2, 4 and 5. Although the antagonist induced slightly larger changes into transmembrane helix 5 than into other transmembrane helices upon binding, the divergence from the apo receptor structure during 150–350 ps of molecular dynamics simulation was more equally distributed among the transmembrane helices than for the full agonist and the partial agonist (Table 3).

The main RMS differences in the transmembrane helices between the agonist bound receptor conformation and the antagonist bound receptor conformation were in transmembrane helix 5 and 6, while the corresponding differences between the agonist bound and partial agonist bound receptor structure were in transmembrane helix 4 and 5 (Table 3). Furthermore, the main differences in the helical

Table 3
RMS difference of receptor domains (backbone atoms) between energy minimised average receptor structures. The complexes are averaged over 150–350 ps of simulation

Receptor domain	Apo receptor/ (*R*)-8-OH-DPAT	Apo receptor/ buspirone	Apo receptor/ (*S*)-WAY100135	(*R*)-8-OH-DPAT/ (*S*)-WAY100135	(*R*)-8-OH-DPAT/ buspirone	Buspirone/ (*S*)-WAY100135
TMH1	0.84	0.66	1.14	1.25	0.67	1.20
TMH2	0.89	1.83	1.21	1.27	1.55	0.93
TMH3	1.62	1.36	1.25	1.31	1.07	1.09
TMH4	1.04	2.33	0.96	0.88	1.92	2.23
TMH5	0.74	1.94	1.39	1.61	2.26	1.24
TMH6	1.77	1.15	1.14	2.22	1.23	1.81
TMH7	1.14	0.91	0.97	1.30	1.22	1.01
IC1	1.35	1.62	1.70	1.53	1.71	1.58
IC2	1.46	1.96	1.36	1.55	1.75	2.04
IC3	5.60	10.20	10.20	9.00	8.70	10.40

Table 4
RMS of fluctuation (backbone atoms) relative to the energy minimised mean receptor structure (150 and 350 ps of simulation)

Receptor domain	RMS of fluctuation			
	Apo receptor	(*R*)-8-OH-DPAT	Buspirone	(*S*)-WAY100135
TMH1	0.48	0.41	0.42	0.40
TMH2	0.49	0.39	0.39	0.42
TMH3	0.44	0.39	0.41	0.39
TMH4	0.59	0.52	0.47	0.41
TMH5	0.53	0.59	0.45	0.51
TMH6	0.48	0.45	0.37	0.41
TMH7	0.40	0.39	0.34	0.37
IC1	0.66	0.51	0.33	0.39
IC2	0.56	0.49	0.37	0.47
IC3	1.23	0.59	0.79	0.75

bundle between the partial agonist complex and the antagonist complex were in transmembrane helix 4 and 6 (Table 3).

During 150–350 ps, molecular dynamics simulation of the apo receptor transmembrane helix 4 and 5 fluctuated more from the average structure than did other transmembrane helices (Table 4). The RMS of fluctuation indicated that transmembrane helix 4 and 5 of the ligand bound receptor structures also fluctuated more from the mean structure during simulation than did other transmembrane helices. The antagonist and the partial agonist constrained the fluctuation of transmembrane helix 4 and 5 more than did the full agonist (Table 4). Interestingly, the agonist seemed to increase the fluctuation of transmembrane helix 5 compared with molecular dynamics simulation of the receptor without any ligand.

Compared with the simulation of the receptor model in absence of a ligand, all ligands seemed to constrain the fluctuations of the intracellular regions (Table 4). Table 4 indicates that (*R*)-8-OH-DPAT constrained the fluctuations of the third intracellular loop more than did buspirone and (*S*)-WAY10035, while (*S*)-WAY10035 and buspirone constrained the fluctuation of the first and second intracellular loop more than did (*R*)-8-OH-DPAT.

4. Discussion

The experimental model of bovine rhodopsin at 2.8 Å resolution, which recently was published (Palczewski et al., 2000), confirmed the suggested α-carbon atom template for G-protein coupled receptors (Baldwin et al., 1997). At 2.8 Å resolution, it is not possible to identify internal hydrogen bonds and side chain torsional angles from the X-ray density map, and the experimental structure must be considered as relatively crude. However, the localisation of highly conserved amino acid residues in the rhodopsin family of G-protein coupled receptors are expected to be similar to that of rhodopsin, and in spite of the relatively low resolution, this experimental structure may serve as a template for further modelling of G-protein coupled receptors.

A successful homology modelling depends strongly upon how closely the structure that is being modelled fits the chosen template. The amino acid identity between backbone atoms in the transmembrane helices of bovine rhodopsin and the human 5-HT_{1A} receptor is about 20 %. An amino acid sequence similarity of 20 % is believed to give a RMS deviation of about 2.0 Å between backbone atoms of the template structure and the target model (Chothia and Lesk, 1986; Hasemann et al., 1995). Structural analysis and visual inspection indicated large similarities between the 5-HT_{1A} receptor model and the experimental rhodopsin structure. (1) The RMS difference between the backbone atoms in the transmembrane helices was 3.0 Å. (2) Highly conserved amino acids in the rhodopsin family of G-protein coupled receptors were located in similar positions and in similar conformations. (3) Large similarities in fragments known to be crucial for activation and ligand binding.

The present 5-HT_{1A} receptor model was based on the suggested α-carbon atom template for G-protein coupled receptors (Baldwin et al., 1997) and not on the recent experimental model of rhodopsin. The generation of this template was assisted by information from a large amount of data on sequences, mutagenesis and biophysical studies. The similarities with the X-ray structure of rhodopsin may be viewed as a validation of the present 5-HT_{1A} receptor model and the methods used in the modelling.

By binding the chromphore retinal in the helical pore and being activated by light, rhodopsin serves functions quite different from those of the neurotransmitter receptors. Although not being a G-protein coupled receptor, bacteriorhodopsin is the bacterial homologue of rhodopsin. However, the helical packing is very different in rhodopsin and bacteriorhodopsin (Palczewski et al., 2000). Therefore, it would also be reasonable to expect that the differences in binding, activation and G-protein coupling mechanisms between the 5-HT_{1A} receptor and rhodopsin would give structural differences in their transmembrane helices. In spite of the fact that the present theoretical model was not based on the experimental model of bovine rhodopsin, we feel that the present 5-HT_{1A} receptor model is as close to reality as a model constructed from the X-ray coordinates of rhodopsin would be. Therefore, the present model may be a useful tool to study the ligand induced dynamical behaviour of 5-HT_{1A} receptor segments.

4.1. Ligand induced conformational changes of the receptor

The average structures from the molecular dynamics simulations provide information about the most populated receptor states in the configurational space explored during the simulations. Therefore, the average receptor structures

after 350 ps of molecular dynamics simulation may provide insight into the structural changes of the receptor upon ligand binding. Based on the results given in Table 3, we suggest that binding of the full agonist induces larger conformational changes into transmembrane helix 3 and 6 than into the other transmembrane helices. This is in agreement with experimental studies of the β_2 adrenergic receptor (Gether et al., 1997; Rasmussen et al., 1999) and the muscarinic M2 receptor (Liu et al., 1996), indicating that receptor activation induces rigid body movements of these transmembrane helices relative to other transmembrane helices. Table 3 indicates that the partial agonist and the antagonist were unable to induce such movements of transmembrane helix 3 and 6 relative to each other as did the full agonist. The main difference in binding mode between the full agonist on one side and the partial agonist and antagonist at the other side was that the full agonist interacted closer to amino acids in transmembrane helix 4 (Fig. 3, Table 2). Site directed mutagenesis studies have shown that the highly conserved proline and tryptophane residues in transmembrane helix 4 are important for activation of the m3 muscarinic receptor (Wess et al., 1993) and the 5-HT_4 receptor (Mialet et al., 2000). This suggests that an interaction between the agonist and transmembrane helix 4 (direct interactions or long range forces) may be important for bringing the agonist and transmembrane helix 4 into position for inducing rigid body movements of transmembrane helix 3 and 6 relative to each other.

The RMS differences in the transmembrane helices between the apo receptor and the antagonist bound receptor indicate that the structural changes upon antagonist binding were equally distributed among the transmembrane helices (Table 3). This may indicate that agonist binding (largest changes into transmembrane helix 3 and 6) and partial agonist binding (largest changes into transmembrane helix 2, 4 and 5) had stronger effects on the helical packing and overall structure of the receptor than binding of the antagonist. The main differences between the agonist bound receptor conformation and the antagonist bound receptor conformation were in transmembrane helix 5 and 6 (Table 3). Similar results were obtained in a molecular modelling study of neuropeptide Y_1 receptor activation (Sylte et al., 1999). This finding is interesting since transmembrane helix 5 and 6 are connected to the third intracellular loop, which is involved in G-protein coupling. This may suggest that the agonist induces changes into transmembrane helix 5 and 6 which creates a proper conformation of the third intracellular loop for G-protein coupling. In spite of the fact that relatively large changes were induced into transmembrane helix 5 by the antagonist, the obtained receptor conformation was far from the agonist bound conformation (Fig. 3). Altogether, the present results suggest that (*S*)-WAY100135 is unable to interact with transmembrane helix 4 in such a way that the required rigid body movements of transmembrane helix 3 and 6 relative to each other may occur.

The RMS of fluctuations during 150–350 ps of simulation with the free receptor indicated that transmembrane helix 4 and 5 fluctuated more from the mean structure than the other transmembrane helices (Table 4). Upon ligand binding the fluctuation of the transmembrane helices and the intracellular loops were constrained (Table 4). The RMS of deviation from the mean structure also indicates that the full agonist constrained the movements of the third intracellular loop more than did the partial agonist and the antagonist (Table 3). This observation indicates that the full agonist constrains the third intracellular loop in a conformation favourable for interactions with the G-protein.

Site directed mutagenesis studies of the gonadotropin-releasing hormone receptor (Sealfon et al., 1995; Flanagan et al., 1999) and the 5-HT_{2A} receptor (Zhou et al., 1994) have shown that an aspartic acid corresponding to Asp^{82} (transmembrane helix 2), and an asparagine corresponding to Asn^{396} (transmembrane helix 7) in the 5-HT_{1A} receptor, are adjacent in space and important for a proper function of the receptor. In the rhodopsin structure, the terminal nitrogen in the side chain of the asparagine (transmembrane helix 7) is located 4.7 Å from one of the terminal oxygens in the aspartic acid (transmembrane helix 2), with a water molecule located in between. The corresponding distance in the 5-HT_{1A} model in absence of ligand was 5.1 Å. Interestingly, the atomic distance between Asp^{82} (transmembrane helix 2) and Asn^{396} (transmembrane helix 7) was increased during simulation with the agonist to 8.1 Å, while the antagonist only slightly increased the distance to 6.1 Å, and the partial agonist decreased the distance to 4.1 Å. After simulation with the agonist, the side chain of Asn^{396} formed hydrogen bonds with the side chain of Ser^{123} (atomic distance 3.0 Å) and His^{126} (atomic distance 3.0 Å) in transmembrane helix 3. After the simulations with the partial agonist and the antagonist, Asn^{396} was hydrogen bonded to the side chain of Ser^{123} (atomic distance: partial agonist 2.1 Å, antagonist 2.3 Å), but not to His^{126}. These results may suggest that agonist-induced displacement of Asp^{82} and Asn^{396} relative to each other formed a hydrogen-bonding network involving both Ser^{123} and His^{126}, which may be important for full receptor activation. However, the possible role of $Ser^{123}$and His^{126} in receptor activation should be verified experimentally.

4.2. A proposed model for receptor activation

The intention with the molecular dynamics simulations was to study the ligand induced conformational changes of the receptor, and not to study how ligands find their way into the active site of the receptor. However, based on the present calculations, and previous calculations with the 5-HT_{1A} receptor (Sylte et al., 1993, 1996), we propose a mechanism for receptor activation. Previous calculations of the 5-HT_{1A} receptor have indicated that the electrostatic potentials are mainly negative around the extracellular

parts and mainly positive around the intracellular parts (Sylte et al., 1996). Furthermore, a region outside Asp^{116} (transmembrane helix 3), which is a key residue for ligand binding (Table 2), forms a negatively charged region at the active site (Sylte et al., 1996). This may suggest that agonist binding to the 5-HT_{1A} receptor is initiated by electrostatic interactions between the negatively charged area outside the extracellular parts and the protonated amino group of the ligand (Fig. 1), and that the negatively charged region near Asp^{116} guides the ligand towards its binding site, most probably by zipper-like mechanisms (Burgen et al., 1975), leading to interactions with key residues in the receptor biding site (Table 2). In order to obtain a complementary complex, rigid body movements of transmembrane helix 3 and 6 relative to each other are induced upon binding of the full agonist, promoting a receptor conformation capable of G-protein recognition. This moves transmembrane helix 5 and 6 into positions leading to a conformation of the third intracellular loop, which favours G-protein interactions. After a stable receptor–agonist complex has been formed, transmembrane helix 4 and 5 fluctuate more than the other transmembrane helices, while the third intracellular loop is constrained in a conformation for high efficacy coupling to G-proteins.

Acknowledgements

This work was supported by computer time on the HP RISC supercomputer at the University of Tromsø, Norway.

References

Arvidsson, L.E., Hacksell, U., Nilson, J.L.G., Hjort, S., Carlsson, A., Lindberg, P., Sanchez, D., Wickstrøm, H., 1981. 8-Hydroxy-2-(di-*n*-propylamino)tetralin, a new centrally acting 5-hydroxytryptamine receptor agonist. J. Med. Chem. 24, 921–923.

Baldwin, J.M., Shertler, G.F.X., Unger, V.M., 1997. An alpha-carbon template for the transmembrane helices in the rhodopsin family of G-protein coupled receptors. J. Mol. Biol. 272, 144–164.

Barnes, N.M., Sharp, T., 1999. A review of central 5-HT receptors and their function. Neuropharmacology 38, 1083–1152.

Bayly, C.I., Cieplak, P., Cornell, W.D., Kollmann, P.A., 1993. A well behaved electrostatic potential based method using charge restrains for deriving atomic charges: the RESP model. J. Phys. Chem. 97, 10269–10280.

Burgen, A.S., Roberts, G.C., Feeney, J., 1975. Binding of flexible ligands to macromolecules. Nature 253, 753–755.

Chanda, P.K., Minchin, M.C.W., Davis, A.R., Greenberg, L., Reilly, Y., Mcgregor, W.H., Bhat, R., Lubeck, M.D., Mizutani, S., Hung, P.P., 1993. Identification of residues important for ligand binding to the human 5-hydroxytryptasmine$_{1A}$ serotonin receptor. Mol. Pharmacol. 43, 516–520.

Chothia, C., Lesk, A.M., 1986. The relation between the divergence of sequence and structure in proteins. EMBO J. 5, 823–826.

Chilmonczyk, Z., Les, A., Wozniakowska, A., Cybulski, J., Koziol, A., Gdaniec, E., 1995. Buspirone analogous as ligands of the 5-HT_{1A} receptor: 1. The molecular structure of buspirone and its two analogous. J. Med. Chem. 38, 1701–1710.

Cliffe, I.A., Brightwell, C.I., Fletcher, A., Forster, E.A., Mansell, H.L., Reilly, Y., Routledge, C., White, A.C., 1993. (*S*)-*N*-*tert*-butyl-3-(4-(2-methoxyphenyl)-piperazin-1-yl)-2-phenylpropanamide [(*S*)-WAY-100135]: a selective antagonist at presynaptic and postsynaptic 5-HT_{1A} receptors. J. Med. Chem. 36, 1509–1510.

Cornell, W.D., Cieplak, P., Bayly, C.I., Gould, I.R., Merz, K.M., Ferguson, D.M., Spellmeyer, D.C., Fox, T., Cadlwell, J.W., Kollmann, P.A., 1995. A second generation force field for the simulation of proteins, nucleic acids, and organic molecules. J. Am. Chem. Soc. 117, 5179–5197.

Christensen, I.T., Jørgensen, F.S., 1997. Molecular mechanical calculations of proteins. Comparison of different energy minimization strategies. J. Biomol. Struct. Dyn. 15, 473–488.

Fanelli, F., Menziani, C., Scheer, A., Cotecchia, S., Benedetti, P.G.D., 1998. Ab initio modeling and molecular dynamics simulation of the α_{1b}-adrenergic receptor activation. Methods 14, 302–317.

Fargin, A., Yamamoto, K., Cotecchia, S., Goldsmith, P.K., Spiegel, A.M., Lapetina, E.G., Caron, M.G., Lefkowitz, R.J., 1991. Dual coupling of the cloned 5-HT_{1A} receptor to both adenylyl cyclase and phosphlipase C is mediated via the same Gi protein. Cell Signalling 3, 547–557.

Farrens, D.L., Altenbach, C., Yang, K., Hubbel, W.L., Khorana, H.G., 1996. Requirement of rigid body motions of transmembrane helices for light activation of rhodopsin. Science 274, 768–770.

Flanagan, C.A., Zhou, W., Chi, L., Yuen, T., Rodic, V., Robertson, D., Johnson, M., Holland, P., Millar, R.P., Weinstein, H., Mitchell, R., Sealfon, S.C., 1999. The functional microdomain in transmembrane helices 2 and 7 regulate expression, activation, and coupling pathways of the gonadotropin-releasing hormone receptor. J. Biol. Chem. 274, 28880–28886.

Gether, U., Lin, S., Ghanouni, P., Ballesteros, J.A., Weinstein, H., Kobilka, B.K., 1997. Agonist induced conformational changes in transmembrane domains III and VI of the β_2 adrenoceptor. EMBO J. 16, 6737–6747.

Gettys, T.W., Fields, T.A., Raymond, J.R., 1994. Selective activation of inhibitory G-protein α-subunits by partial agonists of the human 5-HT_{1A} receptor. Biochemistry 33, 4283–4290.

Guan, X.M., Peroutka, S.J., Kobilka, B.K., 1992. Identification of a single amino acid residue responsible for the binding of a class of β-adrenergic receptor antagonists to 5-hydroxytryptamine$_{1A}$ receptors. Mol. Pharmacol. 41, 695–698.

Hasemann, C.A., Kurumbail, R.G., Boddupalli, S.S., Peterson, J.A., Deisenhofer, J., 1995. Structure and function of cytochromes P450: a comparative analysis of three crystal structures. Structure 3, 41–62.

Hibert, M., Gittos, M.W., Middlemiss, D.N., Mir, A.K., Fozard, J.R., 1988. Grapics computer-aided receptor mapping as a predictive tool for drug design: development of potent, selective, and stereospecific ligands for the 5-HT_{1A} receptor. J. Med. Chem. 31, 1087–1093.

Hibert, M.F., McDermott, I., Middlemiss, D.N., Mir, A.K., Fozard, J.R., 1989. Radiologand binding study of series of 5-HT_{1A} receptor agonists and definition of a steric model of the site. Eur. J. Med. Chem. 24, 31–37.

Ho, B.Y., Karschin, A., Branchek, T., Davidson, N., Lester, H.A., 1992. The role of conserved aspartate and serine residues in ligand binding and in function of the 5-HT_{1A} receptor: a site directed mutagenesis study. FEBS Lett. 312, 259–262.

Karlsson, A., Petterson, C., Sundell, S., Arvidsson, L.-E., Hacksell, U., 1988. Improved preparation, chromatographic separation and X-ray crystallographic determination of the absolute configuration of the enantiomers of 8-hydroxy-2-(dipropylamino)tetralin (8-OH-DPAT). Acta Chem. Scand. B, 42, 231–236.

Kuiper, W., Van Wijngaarden, I., Ijzerman, A.P., 1994. A model of the serotonin 5-HT_{1A} receptor: agonist and antagonist binding sites. Drug Des. Discovery 11, 231–249.

Liu, J., Blin, N., Conklin, B.R., Wess, J., 1996. Molecular mechanisms involved in muscarinic acethylcholine receptor-mediated G protein activation studied by insertion mutagenesis. J. Biol. Chem. 271, 6172–6178.

Mellin, C., Vallgårda, J., Nelson, D.L., Bjørk, L., Yu, H., Andén, N.-E., Csöregh, I., Arvidsson, L.-E., Hacksell, U., 1991. A 3-D model of the 5-HT_{1A} receptor agonist based on stereoselective methyl substituted and conformationally restrictec analogous of 8-hydroxy-2-(dipropylamino)tetralin. J. Med. Chem. 34, 497–510.

Mialet, J., Dahmoune, Y., Lezoualc'h, F., Berque-Bestel, I., Eftekhari, P., Hoebeke, J., Sicsic, S., Langlois, M., Fischmeister, R., 2000. Exploration of the ligand binding site of the human 5-HT_4 receptor by site directed mutagenesis and molecular modeling. Br. J. Pharmacol. 130, 527–538.

Palczewski, K., Kumasaka, T., Hori, T., Behnke, C.A., Motoshima, H., Fox, B.A., Le Trong, I., Teller, D.C., Okada, T., Stenkamp, R.E., Yananoto, M., Miyano, M., 2000. Crystal structure of rhodopsin: a G-prein-coupled receptor. Science 289, 739–745.

Perez, D.M., Hwa, J., Gaivin, R., Mathur, M., Brown, F., Graham, R.M., 1996. Constitutive activation of a single effector pathway: evidence for multiple activation states of a G protein-coupled receptor. Mol. Pharmacol. 49, 112–122.

Peroutka, S.J., 1995. Serotonin receptors: Their evolution and clinical relevance. CNS Drugs 4 (suppl. 1), 18–28.

Rasmussen, S.G.F., Jensen, A.D., Liapakis, G., Ghanouni, P., Javitch, J.A., Gether, U., 1999. Mutation of highly conserved aspartic acid in the β_2 adrenergic receptor: constitutive activation, structural instability, and conformational rearrangement of transmembrane segment 6. Mol. Pharmacol. 56, 175–184.

Raymond, J.R., Olsen, C.L., Getty, T.W., 1993. Cell-specific physical and functional coupling of human 5-HT_{1A} receptors to inhibitory G protein α-subunit and lack of coupling to $G_{s\alpha}$. Biochemistry 32, 11064–11073.

Scheer, A., Cotecchia, S., 1997. Constitutively active G protein-coupled receptors: potential mechanisms of receptor activations. J. Recept. Signal Transduction Res. 17, 57–73.

Sealfon, S.C., Chi, L., Ebersole, B.J., Rodic, V., Zhang, D., Ballesteros, J.A., Weinstein, H., 1995. Related contribution of specific helix 2 and 7 residues to conformational activation of the serotonin 5-HT_{2A} receptors. J. Biol. Chem. 270, 16683–16688.

Sidhu, A., Niznik, H.B., 2000. Coupling of dopamine receptor subtypes to multiple and diverse G proteins. Int. J. Dev. Neurosci. 18, 669–677.

Sylte, I., Edvardsen, Ø., Dahl, S.G., 1993. Molecular dynamics of the 5-HT_{1A} receptor and ligands. Protein Eng. 6, 691–700.

Sylte, I., Edvardsen, Ø., Dahl, S.G., 1996. Molecular modelling of UH-301 and 5-HT_{1A} receptor interactions. Protein Eng. 9, 149–160.

Sylte, I., Chilmonczyk, Z., Dahl, S.G., Cybulski, J., Edvardsen, Ø., 1997. The ligand binding site of buspirone analogous at the 5-HT_{1A} receptor. J. Pharm. Pharmacol. 49, 698–705.

Sylte, I., Andrianjara, C.R., Calvet, A., Pascal, Y., Dahl, S.G., 1999. Molecular dynamics of NPY Y_1 receptor activation. Biorg. Med. Chem. 7, 2737–2748.

Unger, V.M., Hargrave, P.A., Baldwin, J.M., Schetler, G.F.X., 1997. Arrangement of rhodopsin transmembrane alpha-helices. Nature 389, 203–206.

Wess, J., Nanavatia, S., Vogel, Z., Maggio, R., 1993. Functional role of proline and trypthopane residues highly conserved among G-protein coupled receptors studied by mutational analysis of the m3 muscarinic receptor. EMBO J. 12, 331–338.

Zhou, W., Flanagan, C., Ballesteros, J.A., Konvicka, K., Davidson, J.S., Weinstein, H., Miller, R.P., Sealfon, S.C., 1994. A reciprocal mutation supports helix 2 and helix 7 proximity in the gonadotropin-releasing hormone receptor. Mol. Pharmacol. 45, 165–170.